COMBINED BUNDLE ADJUSTMENT OF MOC STEREO IMAGES AND MOLA ALTIMETRY DATA FOR PRECISE MARS TOPOGRAPHIC MAPPING

Jong-Suk Yoon   Jie Shan

Geomatics Engineering, School of Civil Engineering, Purdue University
550 Stadium Mall Dr., West Lafayette, IN 47907-2051, USA
yoon5@ecn.purdue.edu

Commission IV, WG IV/9

ABSTRACT:

Launched in 1996, Mars Global Surveyor (MGS) carries two types of mapping equipments: Mars Orbiter Laser Altimeter (MOLA) and Mar Orbiter Camera (MOC). MOLA collects accurate laser altimetry data over the Mars surface, while MOC acquires high resolution images. In the process of MOLA registration to MOC images, a certain systematic shift was reported in previous studies. This shift may possibly be attributed to time drift when determining the MOC image orientation. To correct such mis-registration and obtain accurate point determination, a bundle adjustment is developed and implemented in this paper. This is a generalized combined adjustment for images collected by pushbroom cameras. Primary participants in this process are MOLA ground points and ranges, MOC image orientation data, and tie points collected on MOC stereo images. As the outcome of the bundle adjustment, we obtain refined MOLA ground points, ground position of tie points, refined MOC image orientation, and an accurate and consistent registration between MOC images and MOLA data. The refined outcome can then be used to generate local and high resolution digital elevation model.

1. INTRODUCTION

Mars topographic mapping products have been generated since 1960's when Mars exploration started to continuously support future exploration plans and scientific research. Recently, studies about Martian topography have become more attractive with new developments in exploration technology. To support the very recent Mars Exploration Rover (MER) missions along with current twin rovers, Spirit and Opportunity, the topography of landing sites has been studied using accumulated data from Mariner to Viking missions and to the latest Mars mapping satellite, Mars Global Surveyor (MGS). This study proposes a bundle adjustment for precise Mars topographic mapping to support the landing site study for the very recent MER missions along with the current twin rovers.

The primary MGS mission objectives are to collect data about Martian surface, atmosphere and magnetic properties and to build a comprehensive dataset for future mission planning (Albee et al., 2001). MGS mapping instruments include Mars Orbiter Laser Altimeter (MOLA) and Mars Orbiter Camera (MOC). MOLA data is considered to be the most accurate mapping data at present with absolute accuracy around 10 meters vertically and around 100 meters horizontally (Kirk et al, 2002). MOC, a linear pushbroom sensor system, provides up to 1.4-meter high resolution images with its narrow angle (NA) camera and 280-meter low resolution images with its wide angle (WA) camera in blue and red bands.

MGS data processing is a challenging task. Anderson and Parker (2002) aligned MOLA profiles to MOC images by empirically matching topographic features for MER landing sites. Ivanov and Lorre (2002) compared MOLA topography from MOC WA and NA stereo pairs of MER landing sites. They report the topography from MOC WA is consistent with MOLA topographic morphology. This paper will present combined adjustment results using high-resolution MOC images, laser altimetry data and MGS trajectory data for precise Mars topographic mapping.

Our approach can be briefly summarized as follows. As the first step, MOLA registration to MOC images is carried out in the previous research (Shan et al. 2004). It showed that the same MOLA points are located on different features in the MOC stereo images. This mis-registration is found nearly to be a constant shift mainly along the flight direction. Next, we present a bundle adjustment to improve the registration quality with the contribution of tie points. Additionally, credible MOLA ranges and MOLA ground coordinates are also included in the bundle adjustment. Mathematical models of measurements and *a priori* statistics are thoroughly presented. Finally, this paper evaluates bundle adjustment results.

This research proposes a new approach to utilize altimetry data, trajectory data and high resolution image data for MGS mapping data processing. The determination of ground points proposed in this research is useful to provide sufficient and accurate ground points for high-resolution elevation model generation.

2. STUDY SITES AND MGS MAPPING DATA

MGS mapping data in this study are chosen from three candidate landing sites of MER missions: Eos Chasma, Gusev Crater and Isidis Planitia. Based on scientific researches, final landing sites are selected by potential scientific values for past liquid water activities and engineering safe landing conditions for MER twin rovers (Savage and Webster, 2003). Among these candidate landing sites, Gusev Crater is finally chosen as the final landing site for Spirit which is one rover of the MER missions launched in 2003 summer. Isidis Planitia is chosen as a backup landing site.

The data include MOC NA images, MOLA profile and MGS trajectory data. MOC is a linear pushbroom scanner taking one line of an image at a time (Albee et al., 2001). The NA camera with 2048 detectors and 3.5 m focal length acquires high-resolution images with 1.4 meter/pixel at nadir. Stereopair of high-resolution images from the NA camera are used for this study. Table 1 illustrates the properties of high-resolution MOC stereo pair images based on the three study sites. The stereo geometry of MOC is across track configuration with one small emission angle for one nadir image and one large emission angle for the other off-nadir image. Line exposure time is a quite important property for the processing of linear pushbroom images. Images are acquired from an acquisition time at the rate of the line exposure time. The image acquisition time in Table 1 shows all images are taken between March and May 2001. Line exposure times and ground space distances (GSD) are different for every image as illustrated in Table 1. Ground space distance indicates the ground distance per pixel, and varies from 3.3 meter/pixel to 5.5 meter/pixel depending on the image.

Table 1. Properties of MOC stereo images

Site Name	Eos Chasma		Gusev Crater		Isidis Planitia	
Image Name	E02 02855	E04 01275	E02 00665	E02 01453	E02 01301	E02 02016
Emission Angle (°)	0.16	17.97	0.2	22.1	13.0	0.2
Acquisition Date (2001)	Mar.31	May 18	Mar. 8	Mar. 17	Mar.15	Mar. 23
Exposure Time (ms)	1.8078	1.2052	1.4462	1.4462	0.9642	1.4462
File Size (H*W)	9856 *672	7424 *1024	10112 *1024	8960 *1024	7680 *1024	7680 *1024
GSD (m/pixel)	5.5	4.1	4.4	4.9	3.3	4.4

MOLA is designed to understand global three-dimensional topography and atmosphere around Mars using laser signals (Smith et al, 2001). If MOLA data and MOC images are obtained at the same time, the MOLA profiles are called simultaneous MOLA profiles. Thus, one MOC image has one linear-pattern MOLA profile and this study uses the simultaneous MOLA profiles of each image. Among several standard MOLA data products, this study is based on Precision Experiment Data Record (PEDR) data generated using precision orbit data. PEDR data consists of areocentric longitude and latitude, range, planetary radius, topographic height, and ephemeris time. Figure 1 shows the MOLA ranging principle in measuring distance between MGS and a footprint of laser signal on the surface. The range is calculated from the time-of-flight of laser pulses and the vacuum speed of light (Abshire et al, 1999). In Figure 1, planetary radius, R_MGS and R_areoid indicate the distances from the center of Mars to the surface, MGS and areoid respectively. Areoid is the reference surface on Mars. Topographic height can be calculated using geometry in Figure 1 (Abshire et al, 1999). The ephemeris time is the time instant that a laser signal is shot. Along with the information provided in PEDR, 3-D ground coordinates, X, Y and Z, of MOLA profiles in Mars body-fixed system, IAU 2000 reference system, can be derived from areocentric longitude and latitude (Shan et al. 2004).
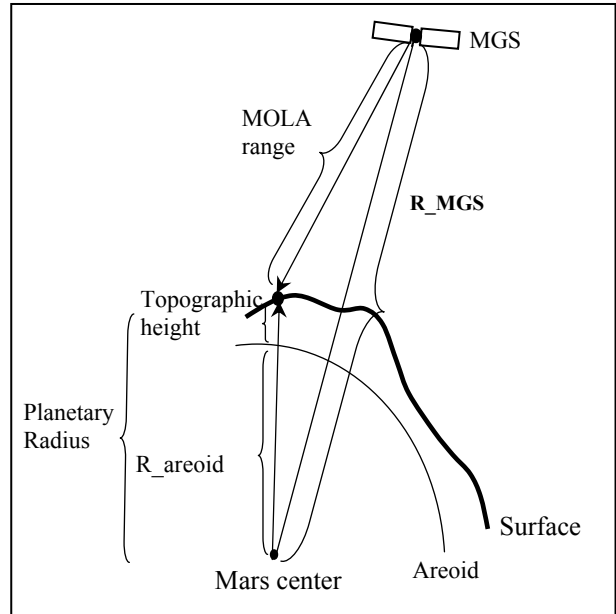

Figure 1. MOLA range, topographic height and planetary radius

3. CONSISTENCY OF MOLA AND MOC REGISTRATION

The property of linear pushbroom images and collinearity equations are used for the calculation of MOC image coordinates of MOLA points. The registration of MOLA, which is a precedent step of this research, is reported in (Yoon and Shan, 2003). For the convenience of readers, this process is briefly summarized. First, MOC exterior orientations are extracted at a constant time interval from SPICE (Spacecraft, Planet, Instrument, C matrix (rotation) and Event) that is a library provided by NAIF NASA. Using SPICE, binary navigation data as it is called a kernel can be accessed by time. Time-dependent exterior orientation of each MOC scan line is modeled by a second order polynomial (Shan et al, 2004). Secondly, image coordinates of corresponding MOLA profiles are calculated using the collinearity equations with the exterior orientation from the sensor model and the ground coordinates of MOLA profiles.

The result of the above calculation shows MOLA profiles are registered into different positions on the two stereopair images. It was previously reported that the registration shifts are around 325 meters mainly in the flight direction in all three study sites. The results are shown in Figure 2 and Figure 3 to compare with bundle adjustment results. To precisely correct this mis-registration and obtain accurate point determination, a bundle adjustment is developed and implemented.

4. BUNDLE ADJUSTMENT

The combined adjustment integrates primarily MOLA profiles, MOC image orientation data, and tie points collected on MOC stereo images. Various types of measurements and their *a priori* standard deviations are introduced in the bundle adjustment. Image coordinates of MOLA and tie points, MOLA ranges, MOLA ground coordinates, MOC exterior orientation are considered as measurements in the bundle adjustment. Image coordinates of MOLA footprints initially result from the previous registration procedure, while image coordinates of tie points are manually and automatically measured on stereo

images. Additionally, MOLA PEDR provides MOLA ranges measured by laser signals. MOLA ground coordinates in Mars body fixed system, X, Y and Z, are derived from latitude and longitude provided from MOLA PEDR as explained before. Exterior orientation parameters are the coefficients of the second polynomial sensor model. Among enumerated types of measurements in the bundle adjustment, image coordinates of tie points, MOLA ground coordinates and MOLA ranges retain high weights to strengthen the adjustments. Following will illustrate mathematical models and *a priori* standard deviations according to each type of measurements in the bundle adjustment.

4.1 Image coordinates of MOLA and tie points

Equation 1 presents the collinearity equations that are applied to every image point. Image coordinates x_i and y_i are related to ground coordinates, X_i, Y_i and Z_i, and exterior orientation parameters in the collinearity equations. Since a MOC image is a linear pushbroom image, the exterior orientations, X^c_{ij}, Y^c_{ij} and Z^c_{ij} and $m_{11} \ldots m_{33}$, are different at each scan line and x_i should be 0 when the exterior orientation is precise.

$$
\begin{aligned}
F_x &= F(EQ\ X_i, Y_i, Z_i) \\
&= x_i + f_j \frac{m_{11}(X_i - X^c_{ij}) + m_{12}(Y_i - Y^c_{ij}) + m_{13}(Z_i - Z^c_{ij})}{m_{31}(X_i - X^c_{ij}) + m_{32}(Y_i - Y^c_{ij}) + m_{33}(Z_i - Z^c_{ij})} = 0 \\
F_y &= F(EQ\ X_i, Y_i, Z_i) \\
&= y_i + f_j \frac{m_{21}(X_i - X^c_{ij}) + m_{22}(Y_i - Y^c_{ij}) + m_{23}(Z_i - Z^c_{ij})}{m_{31}(X_i - X^c_{ij}) + m_{32}(Y_i - Y^c_{ij}) + m_{33}(Z_i - Z^c_{ij})} = 0
\end{aligned}
\tag{1}
$$

where, x_i and y_i are image coordinates of ith point
X_i, Y_i and Z_i are ground coordinates of ith point
X^c_{ij}, Y^c_{ij} and Z^c_{ij} are exterior orientation of ith point of jth image
$m_{11} \ldots m_{33}$ are components of rotation matrix
f_j is focal length of jth image

Image coordinates of MOLA are calculated in the above equations, while tie points are measured on the images. They are treated differently by assigning different *a priori* standard deviations. Image coordinates of tie points are as accurate as one pixel. In the bundle adjustment, the image coordinates variance of tie points is taken as the reference variance, σ_0, and the weight value of the image coordinates is one. *A priori* standard deviations of image coordinates of MOLA profiles are based on the previous analysis about the MOLA registration.

4.2 MOLA ranges

MOLA ranges are incorporated into the bundle adjustment as measurements. The ranges provided in the MOLA PEDR can be formularized by Euclidean distance as a function of camera position and the MOLA footprint as shown in Equation 2. Only simultaneous MOLA profile provides the range information, thus, the range measurement is applied only to the corresponding simultaneous MOC image in the bundle adjustment.

$$
\begin{aligned}
F_{range} &= F(X^c_{ij}, Y^c_{ij}, Z^c_{ij}, X_i, Y_i, Z_i) \\
&= range\ - \sqrt{(X^c_{ij} - X_i)^2 + (Y^c_{ij} - Y_i)^2 + (Z^c_{ij} - Z_i)^2} = 0
\end{aligned}
\tag{2}
$$

where, *range* is from MOLA PEDR file
X^c_{ij}, Y^c_{ij} and Z^c_{ij} are exterior orientation of ith point of jth image
X_i, Y_i and Z_i are ground coordinates of ith points

Abshire et al. [1999] reported MOLA range uncertainty is about 7 meters for a 400 km average range at nadir pointing. MOLA ranges are introduced in the bundle adjustment with 10 meters *a priori* standard deviation.

4.3 Exterior orientation

Exterior orientations extracted from SPICE at a certain time interval are used to model exterior orientations over a MOC image by a second order polynomial. The exterior orientations of each scan line can be estimated using the polynomial function according to the row of an image, x, as shown in Equation 3.

$$
\begin{array}{ll}
X^c_{ij} = a_0 + a_1\ x + a_2\ x^2 & \omega^c_{ij} = d_0 + d_1\ x + d_2\ x^2 \\
Y^c_{ij} = b_0 + b_1\ x + b_2\ x^2 & \varphi^c_{ij} = e_0 + e_1\ x + e_2\ x^2 \\
Z^c_{ij} = c_0 + c_1\ x + c_2\ x^2 & \kappa^c_{ij} = f_0 + f_1\ x + f_2\ x^2
\end{array}
\tag{3}
$$

where X^c_{ij}, Y^c_{ij} and Z^c_{ij} are the sensor position
ω^c_{ij}, φ^c_{ij} and κ^c_{ij} are the sensor pointing
$a_0 \ldots f_2$ are the coefficients of the second order polynomial
x is the line number of the image

Exterior orientation elements are treated as weighted parameters in the bundle adjustment and each variable in Equation 3 will form an additional equation like Equation 4.

$$
F_{EO} = EO - EO^{\circ\circ} = 0
\tag{4}
$$

where, EO stands for the exterior orientation parameters and the polynomial coefficients.

Based on our best knowledge on the accuracy of trajectory data, *a priori* standard deviation of exterior orientation is estimated as the level of 100 and 200 meters. An image with a small emission angle, a nadir image, is assigned 100 meters standard deviation while the off-nadir image with a large emission angle is assigned larger, 200 meters, standard deviation.

4.4 Ground coordinates

MOLA ground coordinates derived from MOLA profiles are input to the bundle adjustment with relatively small *a priori* standard deviations because the coordinates are considered as quite accurate data source. Therefore, *a priori* standard deviations of MOLA ground coordinates are set at the level of 10 meter for each X, Y, and Z coordinates. Ground coordinates of tie points are treated as free unknowns, namely, those have practically infinity as *a priori* standard deviation. Ground points will form the following observation equations

$$
F_{ground} = XYZ - XYZ^{\circ\circ} = 0
\tag{5}
$$

where, XYZ stands for the ground coordinates.

Based on standard deviations, the measurements' weights are assigned. In this study, *a priori* standard deviation of image coordinates of tie point is taken as reference variance with unit weight, 1.

5. RESULTS AND EVALUATION

This section presents and evaluates the results of the bundle adjustment. First, the amount of correction of measurements is examined in three sites according to the types of measurements. Secondly, error propagation is theoretically computed, namely, the variances of ground coordinates are calculated from the normal equations in the least squares solution. Last, the MOLA registration is carried out using adjusted exterior orientation coefficients, and the improved registration results are visually presented.

5.1 Corrections and residuals

Table 2 presents the amount of correction of ground coordinates. Overall, average correction of tie points is larger than those of MOLA profiles. Because MOLA ground coordinates are treated with relatively high weights in the bundle adjustment, the corrections of MOLA ground coordinates show from 4 mm to 0.1 mm in all three sites. That means the MOLA ground coordinates are almost not changed. For differences among sites, the ground coordinate corrections of tie points show small changes in Gusev Crater and Isidis Planitia sites, but in Eos Chasma site, the corrections of tie ground coordinates show 91m, 107m and 55m in X, Y, and Z respectively. Furthermore, RMSs of ground coordinates are so small that the corrections of all points are quantitatively similar except tie points in Eos Chasma. Therefore, the ground coordinates of tie points in Eos Chasma are adjusted quite large amount and the corrections show large differences among the tie points as well.

Table 2. Statistics of ground coordinates correction (in meters)

Site	Type	X (Mean /RMS)	Y (Mean /RMS)	Z (Mean /RMS)
Eos Chasma	MOLA	0.001/0.256	-0.001/0.366	0.004/0.188
	Tie	-91.232 /117.676	106.913 /151.426	54.799 /59.585
Gusev Crater	MOLA	-0.001/0.299	0.001/0.098	0.001/0.135
	Tie	-1.794/2.723	0.371/0.340	6.750/1.10
Isidis Planitia	MOLA	0.0004/0.056	0.0001/0.222	0.023/0.746
	Tie	0.222/0.189	-1.786/1.011	3.144/3.148

The reason of the manifest differences in Eos Chasma is presumed to be caused by the image acquisition date difference. Navigation data for exterior orientation, kernel, are determined according to each image acquisition time. In Eos Chasma site, unlike other two study sites, the two stereo pair images are acquired on quite different dates; one image from March 2001 and the other from May 2001. In this case, different navigation data are used to estimate sensor orientation and position for each image. Because exterior orientation from two different MGS orbits is inconsistent with each other, Eos Chasma shows incompatible results with other two study sites.

In Table 3, the amount of correction and residuals of image coordinates are large in *x* image coordinates in all three sites, which mean image coordinates are mainly changed along the flight direction. Consequently, the reported MOLA mis-registration along the flight direction in the previous research is corrected after the bundle adjustment. This is later proven with figures showing MOLA profiles overlaid with MOC stereo images. The image coordinates of tie points showing relatively quite small residuals are not changed at all on the images of all sites. The results of Gusev Crater and Isidis Planitia show similar pattern: large amount of correction in *x* direction, small amount of correction in *y* direction and small RMS in both directions. In the Eos Chasma site, however, RMSs of MOLA image corrections have a large variance in both directions. The different pattern in Eos Chasma site can be explained by the same reason presented before.

Table 3. Statistics of image coordinates: correction for MOLA profiles and residuals of tie points (in pixels)

Site	Type	Image 1		Image 2	
		x Mean /RMS	*y* Mean /RMS	*x* Mean /RMS	*y* Mean /RMS
Eos	MOLA	12.789 /61.724	4.040 /15.915	-8.419 /-18.116	47.103 /40.515
	Tie	-0.009 /0.615	-0.002 /0.055	0.009 /0.418	-0.002 /0.030
Gusev	MOLA	-24.176 /0.774	3.286 /0.254	24.895 /0.104	-2.695 /0.163
	Tie	0.086 /0.603	-0.012 /0.084	-0.089 /0.621	0.009 /0.069
Isidis	MOLA	35.044 /0.082	-2.711 /0.198	-24.789 /1.519	2.891 /0.357
	Tie	-0.162 /0.453	0.012 /0.035	0.119 /0.322	-0.018 /0.038

MOLA ranges play a role of constraining the geometric relationship between exterior orientation and ground coordinates. Residuals of MOLA ranges vary from about 1 meter up to about 2 meters. Along with other measurements, exterior orientation coefficients are also adjusted through the bundle adjustment. MOLA and MOC registration results presented later will show the effect of adjusted exterior orientation coefficients.

5.2 Theoretic analysis

A posteriori reference standard deviations ($\hat{\sigma}_0$) are computed from the residuals of measurements. In all three study sites, *a posteriori* reference standard deviations are close to *a priori* ($\sigma_0 = 1$) reference standard deviations: 1.037, 1.059, and 1.014 pixels as shown in Table 4.

Subsequently, *a posteriori* standard deviation is used to compute the variance-covariance of the ground coordinates of MOLA and tie points. Table 4 shows the standard deviations of the ground coordinates of MOLA and tie points. Generally, the standard deviations of MOLA profiles show relatively smaller than those of tie points. *A posteriori* standard deviations of MOLA points are consistent with *a priori* estimation, 10 meters. In the Eos Chasma site, the standard deviations of tie ground coordinates are lager than the standard deviations of MOLA points and the magnitudes are quite larger than those of other two sites.

Table 4. Standard deviations of the adjusted ground coordinate of MOLA and tie points

Site	Type	σ_X (m)	σ_Y (m)	σ_Z (m)	$\hat{\sigma}_0$ (pixel)
Eos Chasma	MOLA	9.210	8.941	10.183	1.037
	Tie	99.012	141.643	43.296	
Gusev Crater	MOLA	7.869	10.205	10.158	1.059
	Tie	21.270	5.020	6.633	
Isidis Planitia	MOLA	18.297	9.799	18.302	1.014
	Tie	7.344	57.934	8.684	

5.3 MOLA and MOC Registration

The image coordinates of MOLA ground points are calculated using adjusted exterior orientation coefficients after the bundle adjustment. The new image coordinates can be compared with the mis-registered image coordinates of MOLA profiles obtained before bundle adjustment to examine the improvement as a result of the bundle adjustment.

The improvement of the MOLA registration can be examined by visual checks in Figure 2 and Figure 3. Figure 2 shows the comparison of the MOLA profile registration on stereo images before and after the bundle adjustment in Gusev Crater site. The results of all sites show considerable improvement of MOLA registration. However, only Gusev Crater (Figure 2) and Isidis Planitia (Figure 3) results are provided due to the limit of space. Figure 2 (a) images are the MOLA profile registration overlaid with MOC stereo pair images before bundle adjustment. The MOLA profiles show the systematic registration shifts around one MOLA GSD, about 325 meters, in both stereo pair images. The index number 77 of MOLA profile is projected outside of a crater in the left stereo pair image and, inside of the crater in the right stereo pair image in Figure 2 (a). Figure 2 (b) images are the MOLA profile registration after the bundle adjustment with the contribution of tie points, MOLA ranges and other measurements. Figure 2 (b) is the MOLA registration after the bundle adjustment using new adjusted exterior orientation. The MOLA profile with index number 77 is projected to the same positions slightly outside of the crater on the both stereo pair images. Figure 3 shows MOLA registration to MOC stereo images in Isidis Planitia. Figure 3 shows the MOLA registration results before (Figure 3 (a)) and after (Figure 3 (b)) bundle adjustment in Isidis Planitia. Figure 3 also shows MOLA profile with index numbers near a crater in Isidis Planitia site to easily identify the MOLA registration results. MOLA profile locations from index 6 to index 8 are different in the stereo pair around the crater area in Figure 3 (a). However, they are correctly projected to the same in Figure 3 (b).

Figure 4 is the bundle adjustment results with MOLA profiles and tie points overlaid with MOC stereo pairs. Figure 4 (a) shows the stereo pair of Gusev Crater site and Figure 4 (b) is the stereo pair of Eos Chasma sate. MOLA profiles show linear pattern on the images, while tie points are scattered over the images. Because the tie points are not changed after the bundle adjustment, it shows exactly the same location as they are collected either manually or automatically. In Figure 4, image coordinates of MOLA and tie points are projected to the same position of both stereo pair images.
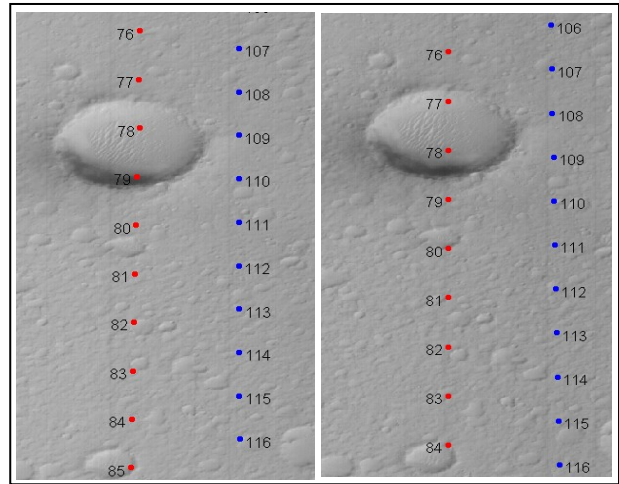

Figure 2 (a). MOLA registration before bundle adjustment in Gusev Crater
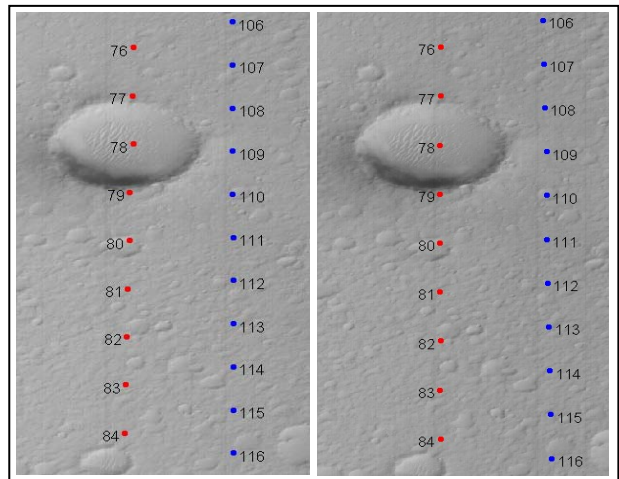

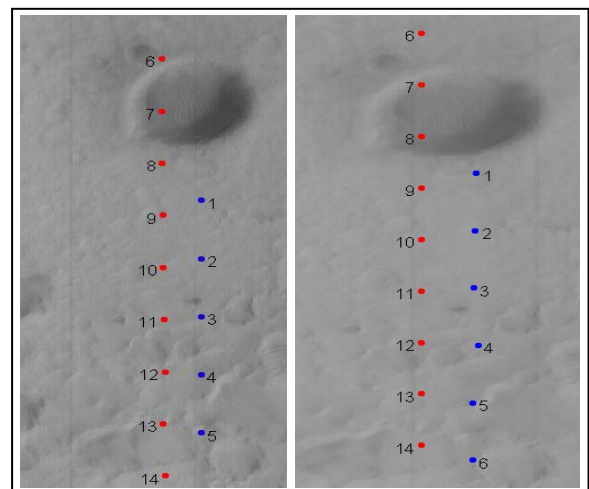Figure 2 (b). MOLA registration after bundle adjustment in Gusev Crater

Figure 3 (a). MOLA registration before bundle adjustment in Isidis Planitia
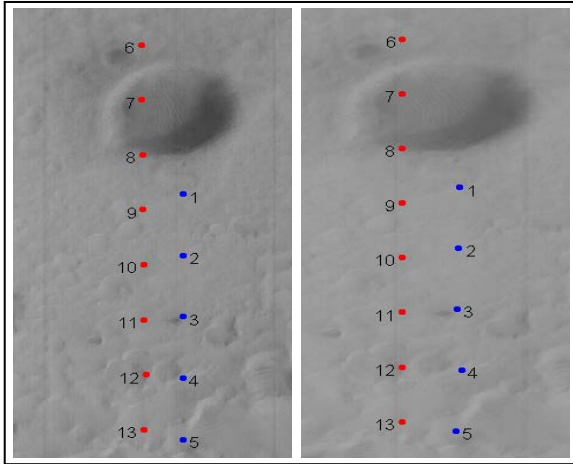
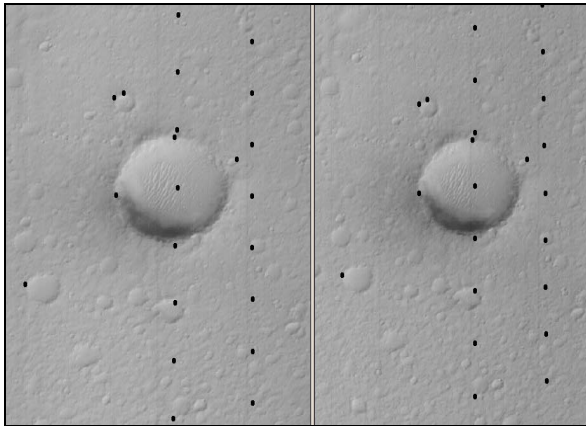Figure 3 (b) MOLA registration after bundle adjustment in Isidis Planitia

Figure 4 (a). MOLA and tie points overlaid with MOC stereo pair after bundle adjustment in Gusev Crater site
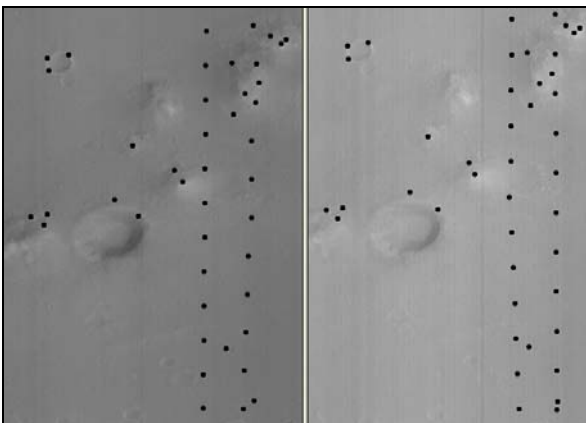

Figure 4 (b). MOLA and tie points overlaid with MOC stereo pair after bundle adjustment in Eos Chasma site

6. CONCLUSIONS

The combined bundle adjustment of MOC stereopair images and MOLA data significantly improves the MOLA-MOC registration. All available types of measurements are incorporated into the bundle adjustment with certain weights. Along with high quality MOLA ranges and ground points,

precise tie image points complement the insufficient MOLA geometry. With these precise measurements, MOC exterior orientations are adjusted. The mis-registration of MOLA that is around 325 meters along the flight direction is removed so that MOLA profiles are registered to the same position on the two stereopair images. Results from all of the three study sites support this conclusion. Consequently, the proposed bundle adjustment can overcome the scarcity of Martian ground control points by a combined processing of MOLA and MOC data under one unified mathematical frame. Our study suggests that handling MGS data collected at considerably different dates may be problematic due to the large inconsistency in the trajectory data.

REFERENCES

Abshire, J.B., X. Sun, and R.S. Afzal, 1999. Mars Orbiter Laser Altimeter: receiver model and performance analysis. NASA Goddard Space Flight Center.

Albee, A.L., R.E. Arvidson, F. Palluconi, and T. Thorpe, 2001. Overview of the Mars Global Surveyor mission. Journal of Geophysical Research, Vol. 106, No. E10, October 25, pp. 23,291-23,316.

Anderson, F.S., and T.J. Parker, 2002. Characterization of MER landing sites using MOC and MOLA. The 33rd Lunar and Planetary Science Conference, March 11–15, League City, TX.

Ivanov, A.B., and J.J. Lorre, 2002. Analysis of Mars Orbiter camera stereo pairs. The 33rd Lunar and Planetary Science Conference, March 11–15, League City, TX.

Kirk, R.L., L.A. Soderblom, E. Howington-Kraus, and B. Archinal, 2002. USGS High resolution topomapping of Mars with Mars Orbiter Camera Narrow-angle Images, IAPRS, Vol.34, Part 4, "GeoSpatial Theory,Processing and Applications", Ottawa, CD-ROM.

Savage, D. and G. Webster, 2003. NASA Rovers Slated To Examine Two Intriguing Sites On MARS, Retrieved 04 23, 2004, from http://marsoweb.nas.nasa.gov/landingsites/mer2003/doc/finalists_selected.html

Shan, J., J-S Yoon, D. S. Lee, L. Randolph, R. L. Kirk, G. A. Neumann and C. H. Acton, 2004. Photogrammetric Analysis of the Mars Global Surveyor Mapping Data. PE&RS (in print).

Smith, D.E., M.T. Zuber, H.V. Frey, J.B. Garvin, J.W. Head, D.O. Muhleman, G.H. Pettengill, R.J. Phillips, S. Solomon, H.J. Zwally, W.B. Banerdt, T.C. Duxbury, M.P. Golombek, F.G. Lemoine, G.A. Neumann, D.D. Rowlands, O. Aharonson, P.G. Ford, A.B. Ivanov, C.L. Johnson, P.J. McGovern, J.B. Abshire, R.S. Afzal, and X. Sun, 2001. Mars Orbiter Laser Altimeter: Experiment summary after the first year of global mapping of Mars, Journal of Geophysical Research, Vol. 106, No. E10, pp. 23,689–23,722.

Yoon, J-S and J. Shan, 2003. Registration and its Uncertainty of MOLA Profiles with MOC Stereo Images. ISPRS WG IV/9 Extraterrestrial Mapping Workshop, Houston, USA.